Engineering Reports

WILEY

Engineering Reports Open Access

RESEARCH ARTICLE OPEN ACCESS

Influence of Nonwoven Geotextiles and Geogrids on Shear Strength of Expansive Montmorillonite Clay

Assel Tulebekova[1] | Zhanar Kusbergenova[1] | Aliya Aldungarova[2] | Gulshat Tleulenova[1] | Dauren Yessentay[3] | Uliya Abdikerova[4] | Nargul Saktaganova[4] | Atogali Jumabayev[1] | Timoth Mkilima[5]

[1]Department of Civil Engineering, L.N. Gumilyov Eurasian National University, Astana, Kazakhstan | [2]School of Engineering, International Educational Corporation, Almaty, Kazakhstan | [3]Department of Transport Construction and Production of Building Materials, Kazakh Automobile and Road Institute, Almaty, Kazakhstan | [4]Institute of Engineering and Technology, Department of Architecture and Construction Production, Korkyt Ata Kyzylorda University, Kyzylorda, Kazakhstan | [5]Department of Environmental Engineering and Management, The University of Dodoma, Dodoma, Tanzania

Correspondence: Timoth Mkilima (tmkilima@gmail.com)

Received: 3 May 2025 | **Revised:** 17 May 2025 | **Accepted:** 18 June 2025

Keywords: cohesion | geogrids | geosynthetic | shear stress | soil mechanics

ABSTRACT

Geosynthetic reinforcement plays a crucial role in stabilizing subgrade layers and enhancing the bearing capacity of soil in construction projects. Despite notable advancements in soil reinforcement techniques, there remains a lack of comprehensive understanding regarding the interactions between various geosynthetic materials and different soil types. This study investigates the effectiveness of different geosynthetic reinforcements in enhancing the shear strength of expansive montmorillonite clay. The research aims to compare the performance of two reinforcement types (biodegradable geocell and a nonwoven geotextile) against a conventional woven geogrid, assessing their influence on soil stability under various stress conditions. Reinforcing the expansive montmorillonite clay with either nonwoven geotextiles or geogrids effectively increased its shear strength under various normal stress levels. For example, at a normal stress of 100 kPa, geogrid reinforcement increased the shear strength from 50 kPa (unreinforced) to 65.5 kPa, while nonwoven geotextiles resulted in a shear strength of 51.2 kPa, highlighting the superior performance of geogrids in enhancing soil stability. Additionally, the use of nonwoven geotextile was found to enhance cohesion from 8 to 15 kPa. When exposed to moisture, the unreinforced soil expanded significantly, exhibiting a swelling strain of 12.8%. However, reinforcing the soil with biodegradable geocells (GC) substantially mitigated this expansion, reducing the swelling strain to 4.2%. While woven geogrids also limited swelling (7.5% strain), they were not as effective as the biodegradable geocells in minimizing volumetric changes.

1 | Introduction

Soil reinforcement is a set of measures aimed at improving the soil's physical and mechanical properties to ensure building structures' stability and durability. Different soil reinforcement methods are used depending on the soil type, geological conditions, and project requirements [1]. Today, physical, mechanical, and chemical soil reinforcement methods are widely used [2]. Mechanical soil reinforcement methods involve utilizing physical actions to enhance the properties of soil. These methods of improving soil are without changing its chemical composition [3, 4]. Features of mechanical methods include the use of various machines, equipment, and technologies to achieve the desired results. Each of the presented methods has its peculiarities, loading is characterized by the absence of the need for special mechanization, and there is a possibility to accelerate secondary

settlement, but the disadvantage is high labour intensity [5]. For others: vibrating; low operating noise, ease of operation, maneuverability but the ground must have optimum moisture content and the density of the ground is not uniform in depth [6]; tramming; the simplicity of the method, the possibility of application in winter conditions but rapid wear of winch mechanism and cables; explosions; the possibility of quick compaction, low cost but there is a need to ensure the moisture content of soils, uneven compaction by layer thickness, limited application near buildings and structures.

In construction and geotechnical engineering, expansive montmorillonite clay, characterized by its high swelling potential and low shear strength, poses significant challenges to stability and performance [7]. This type of clay often leads to issues such as foundation heave, shrinkage-induced cracking, and differential settlement, necessitating effective reinforcement strategies to mitigate volume changes and ensure structural integrity [8]. This study addresses these challenges by investigating the effectiveness of various geosynthetic reinforcements; specifically, a novel biodegradable geocell, a nonwoven geotextile, and a conventional woven geogrid. By comparing these reinforcement materials under different stress and moisture conditions, the research aims to provide valuable insights into their potential for enhancing the shear strength, load distribution, and deformation control of expansive clay. Understanding how these materials perform can significantly impact design and construction practices, leading to more resilient infrastructure and improved mitigation of swelling-induced damage. This study's findings are crucial for advancing knowledge in expansive soil reinforcement and developing practical solutions for real-world engineering challenges.

The use of geosynthetics for soil reinforcement presents several key advantages over traditional methods [9, 10]. These benefits arise from the unique properties of geosynthetics and their effectiveness across various conditions [11, 12]. Consequently, there is extensive research on geosynthetic applications. Studying different conditions is crucial for understanding the performance and effectiveness of reinforced soil structures under varying stress orientations [13]. It is important to note that the behavior of reinforced soils under varying shear conditions is critical for understanding stability and performance in geotechnical applications. When shear forces act along the plane of the reinforcement, frictional resistance and load transfer capabilities between the soil and reinforcement play a key role in enhancing shear strength, as shown in studies evaluating geosynthetics in low- and medium-plastic cohesive soils. Conversely, when shear forces are applied perpendicular to the reinforcement layer, the ability of the reinforcement to resist pullout forces and maintain stability becomes crucial. Experimental findings reveal that woven geotextiles outperform other reinforcements due to their superior interface frictional resistance and tensile strength, particularly in soils with low plasticity, where shear strength and cohesion increased by over 200% compared to unreinforced soils [14]. However, in higher plastic soils, the performance of reinforcements declines due to reduced interface friction and interlocking effects, highlighting the importance of soil–reinforcement interaction in determining effectiveness.

Also, the results of many studies show the changes in the strength and deformation properties of soil reinforced with geosynthetic materials at different degrees of water saturation [15, 16]. The test results are also significantly influenced by the specimen preparation procedure for the shear test, especially for the mixed samples. The studies noted that the dry pluviation method cannot guarantee a homogeneous and saturated specimen of sand–clay mixture or well-graded sand; the wet pluviation cannot be used for well-graded soil or sands containing fine particles because of the particle segregation [17]; dry tamping sample preparation can successfully avoid the honeycomb structure [17, 18] induced by the capillary forces, but it enhances the heterogeneities and uncertainty of physical properties in the sand-clay mixture specimens due to the possible segregation effect; consolidation of the sand-clay mixture slurry on the interface direct shear device may result in soil leakage. Research into additional parameters affecting soil testing results through direct shear tests is ongoing. Despite considerable advancements in soil reinforcement, knowledge about the interactions between various geosynthetic materials and soil types remains limited. While previous studies have underscored the advantages of different reinforcement methods, there is a lack of comprehensive analyses examining their effectiveness under diverse conditions. Particularly, the information on the potential of biodegradable geocell and woven geogrid in expansive montmorillonite clay is still scarce, making this study a valuable contribution to the understanding of their effectiveness in soil reinforcement. This study introduces a novel comparative assessment of horizontal, dual-horizontal, and vertical orientations of multiple geosynthetic types, including a biodegradable geocell within expansive montmorillonite clay, providing new insights into configuration-dependent reinforcement mechanisms that have not been systematically investigated in previous small-scale shear testing studies.

2 | Materials and Methods

As noted earlier, this study examined how different geosynthetic reinforcements affect the shear strength of expansive montmorillonite clay. The objective was to compare the performance of two types of reinforcements, a new biodegradable geocell and a nonwoven geotextile, against a traditional woven geogrid. The focus was on evaluating their impact on soil stability under a range of stress conditions.

2.1 | Material Properties

2.1.1 | Geosynthetic Reinforcements

The biodegradable geocell used in this study featured a three-dimensional honeycomb structure crafted from a woven blend of 70% jute fibers and 30% coir fibers. The geocell had a mass per unit area of 350 g/m^2, with individual cells measuring 100 mm in diameter and 50 mm in height. The jute/coir fabric was fabricated using traditional handloom weaving techniques, and the cells were joined using a specialized biodegradable polyester thread (manufactured by Coats EcoVerde). The geocell demonstrated a tensile strength of 3.5 kN/m, flexibility with a bending stiffness of 1.2 N m, and biodegradability with a 60% mass loss over 12 months under natural soil conditions. The tensile strength of the geocell was determined following the provisions of ASTM D6637/D6637M-15: Standard Test Method

for Determining Tensile Properties of Geogrids by the Single or Multi-Rib Tensile Method, which is widely recognized for geosynthetic material characterization.

The particle size distribution of the dry sample was determined using laser diffraction and wet sieving methods to accurately quantify the distribution of particles across various size fractions (0.1–100 μm) before swelling. Following this, the clay was subjected to controlled swelling by adding distilled water in increments, ensuring complete saturation. During the swelling process, the sample was confined in a sealed container to maintain a constant volume and prevent any external volume change. Particle size measurements were taken at three stages: before swelling (dry state), at constant volume (during swelling), and after swelling (once the clay reached full hydration and expansion). The sample was left to swell for 72 h, allowing the clay to absorb water and expand fully. After swelling, the PSD was re-analyzed using the same methods to assess the redistribution of particles. The data were then compared to determine how the swelling process affected the concentration of fine (< 5 μm) and coarse (> 10 μm) particles. This experimental setup allowed for a detailed examination of the changes in the soil structure due to swelling, providing insights into the potential effects on shear strength, stability, and overall soil behavior.

The nonwoven geotextile used in the research was made from high-strength polypropylene fibers, selected for their chemical and biological resistance, and manufactured through a needle-punching process followed by thermal bonding. This resulted in a durable fabric with a surface density of 400 g/m^2, a tensile strength of 13.0 kN/m, and a relative elongation at break of 55%–130%. It was chosen for its reliability in enhancing soil stability and was tested for permeability (0.01 cm/s), puncture resistance (600 N), and filtration capabilities. For comparison, the conventional woven geogrid (TriAx TX140, supplied by Tensar Corporation) had a mass per unit area of 270 g/m^2 and was made from high-tenacity polyester yarns coated with PVC for increased durability against UV exposure and chemical attack. Its biaxial design, with a triangular aperture structure, helped distribute loads more effectively, improving soil interaction and stabilization. The geogrid had a tensile strength of 35 kN/m (longitudinal/transverse), with a relative elongation at a break of 12% in both directions, making it suitable for soil stabilization applications. It was also tested for junction strength (10 kN), aperture stability, and load-strain behavior.

2.1.2 | Soil

The soil used was an expansive montmorillonite clay sourced from the Almaty region in Kazakhstan. This type of clay was selected due to its well-defined properties and its prevalence in various construction scenarios. The clay was air-dried and sieved through a 2 mm sieve to ensure homogeneity and consistency for testing. Table 1 summarizes the key physical properties of the clay, determined according to relevant ASTM standards.

The air-dried expansive montmorillonite clay was moistened to achieve a consistent moisture content of 12%, corresponding to approximately 85% saturation based on the clay's compaction characteristics. Moisture content was meticulously controlled using an electronic moisture balance (OHAUS MB200) with an accuracy of 0.01%, ensuring precise and uniform moisture levels across all samples. The moist clay was compacted directly into standard shear box molds (6 × 6 × 2 cm) using a hydraulic press (ELE International, ELE-180). A consistent compaction effort was applied to achieve a target dry density of 1.75 g/cm^3, representing 95% of the maximum dry density obtained from standard Proctor compaction tests. For specimens reinforced with geotextiles, the compaction method was adjusted by compacting the clay in layers, with geotextiles placed at predetermined positions within the mold. Each layer was carefully compacted to maintain uniform density, ensuring proper integration of the geotextile reinforcement without disrupting the overall specimen integrity. The compaction target was confirmed by calculating the bulk density of the compacted specimens based on their measured weight and volume. Any specimens deviating by more than ±0.01 g/cm^3 from the target density were discarded and remolded to maintain consistency. This rigorous process minimized variability and ensured uniformity across all specimens, enhancing the reproducibility of the test results. The test strain rate was selected based on ASTM D3080/D3080M standards to ensure compatibility with the drained condition of the expansive montmorillonite clay. A strain rate of 0.2 mm/min was chosen to allow adequate time for pore pressure dissipation, consistent with the requirements for drained shear tests. The maximum strain for each test was set at 10% of the specimen height (6 mm), which was sufficient to capture the peak shear strength and post-peak behavior while avoiding excessive deformation beyond the operational range. A total of 36 samples were prepared for the direct shear tests, with each test configuration repeated in triplicate to ensure statistical significance.

TABLE 1 | Physical properties of the material.

Properties	Value	ASTM standard
Specific gravity (g/cm^3)	2.6	ASTM D854
Maximum dry density (g/cm^3)	1.45	ASTM D698
Optimum water content (%)	20	ASTM D698
Particle size distribution		ASTM D422
Gravel (4.75–2.00 mm)	2%	
Sand (2.00–0.075 mm)	10%	
Silt/clay (< 0.075 mm)	88%	

2.1.3 | Geosynthetic Placement

To investigate the effect of different geosynthetic materials and placement orientations on the shear behavior of expansive soils, a refined testing protocol was employed using a small-scale direct shear apparatus with internal dimensions of 6 × 6 × 2 cm. While compact, this apparatus provides precise control over specimen geometry and allows for rapid, repeatable testing under standardized conditions. The experimental configuration was designed as a foundational step before subsequent large-scale physical modeling and numerical simulations currently under development.

Three distinct reinforcement materials were used:

1. Biodegradable geocell fabricated from 70% jute and 30% coir (mass per unit area: 350 g/m^2; cell size: 100 mm diameter, 50 mm height).

2. Nonwoven geotextile (commercial, polypropylene-based, 200 g/m^2).
3. Woven geogrid (TriAx TX140, Tensar Corp., 140 g/m^2).

Each material was precisely trimmed to match the box dimensions to avoid folding, edge interference, or stress concentration effects.

To simulate a broader range of real-world reinforcement strategies and introduce experimental innovation, three distinct geosynthetic placement configurations were adopted:

1. **Single Horizontal Reinforcement (SHR)**
   The reinforcement layer was placed at mid-height (1 cm from the base) of the compacted expansive montmorillonite clay specimen. This conventional placement aims to intercept the critical shear plane and redistribute applied loads, enhancing lateral resistance.
2. **Dual Horizontal Reinforcement (DHR)**
   Two geosynthetic layers were embedded; one at 0.67 cm and another at 1.33 cm depth, creating a sandwich structure within the soil matrix. This configuration was designed to assess whether distributing reinforcement across multiple interfaces yields improved shear resistance, particularly in thick or multi-layered soil systems.
3. **Vertical Reinforcement Insertion (VRI)**
   Vertical strips of geosynthetic material (6 cm height × 0.5 cm width) were inserted perpendicularly through pre-cut slits in the compacted clay, spaced 1 cm apart. This unconventional orientation mimics deep-rooted vegetation or vertical anchoring systems and was introduced to investigate vertical confinement effects and potential interlocking between soil particles and vertical reinforcement elements.

Each clay specimen was prepared by compacting air-dried montmorillonite clay (sieved through a 2 mm mesh) in two or three layers (depending on configuration) to a target dry density of 1.75 ± 0.02 g/cm^3, using a hand-operated mini-proctor compactor and guided mold to maintain uniformity. Moisture content was fixed at 20% to simulate near-optimum field conditions. To ensure statistical reliability and repeatability, each test configuration and material type was replicated five times ($n = 5$). A total of 45 reinforced specimens (3 configurations × 3 materials × 5 replicates) and five unreinforced control specimens were tested under identical loading and boundary conditions.

2.2 | Direct Shear Test

In the study, the geosynthetic material was fixed in the direct shear test by placing it securely on the base of the shear box, ensuring full coverage under the soil specimen. The edges of the geosynthetic were fastened using adhesive tape to prevent movement during testing. The soil specimen was then carefully placed and compacted over the geosynthetic, and the shear box was assembled before conducting the test to evaluate the soil-geosynthetic interaction. Direct shear tests were conducted in accordance with ASTM D3080 (Standard Test Method for Direct Shear Test of Soils Under Consolidated Drained Conditions) using a model CSU-2 Direct Shear Apparatus from Geotechnical Testing Services. This apparatus is designed to apply controlled normal and shear stresses to soil specimens, allowing for precise measurement of shear strength parameters under consolidated drained conditions. The CSU-2 Direct Shear Apparatus features a robust load frame and advanced data acquisition system, ensuring accurate and reliable results for evaluating the performance of geosynthetic reinforcements in soil stabilization.

2.2.1 | Testing Procedure

Normal Stress Application: The direct shear tests applied three predetermined normal stress levels: 50, 100, and 150 kPa, to the soil specimens. Each stress level was precisely controlled and maintained throughout the shearing process using a pneumatic control system integrated into the CSU-2 Direct Shear Apparatus. This system ensured stable and consistent normal stresses were applied, preventing any fluctuations that could affect the test results.

Shearing: During the shearing phase, the shear box was subjected to a controlled shearing displacement at a constant rate of 1.00 mm/min, achieved using a motorized actuator. This actuator allowed for smooth and accurate application of shear forces, ensuring that the displacement rate was uniform across all tests.

Data Acquisition: Shear force, horizontal displacement, and vertical displacement were continuously monitored and recorded throughout the shearing process. A load cell measured the shear force, while linear variable differential transformers (LVDTs) were used to measure horizontal and vertical displacements. Data acquisition was managed using a Campbell Scientific CR1000 data logger, which recorded data at a sampling rate of 1 Hz. This setup provided high-resolution and accurate measurements necessary for detailed analysis of soil-reinforcement interactions.

2.2.2 | Testing Matrix

Twelve test configurations were investigated in the study to evaluate the effectiveness of various geosynthetic reinforcements. Each configuration was designed to assess the impact of different reinforcement types on the shear strength and stability of expansive montmorillonite clay under controlled conditions. The configurations included:

4. Unreinforced soil: Three replicates were tested at each normal stress level (50, 100, and 150 kPa) to establish baseline shear strength parameters for comparison.
5. Soil reinforced with biodegradable geocell: Three replicates were tested at each normal stress level. The biodegradable geocell was positioned horizontally and perpendicular within the soil specimens to assess its impact on shear strength.
6. Soil reinforced with nonwoven geotextile: Three replicates were tested at each normal stress level. The nonwoven geotextile was placed horizontally and perpendicular to evaluate its effectiveness in enhancing soil stability.
7. Soil reinforced with conventional woven geogrid: Three replicates were tested at each normal stress level. The woven

geogrid was placed both horizontally and perpendicularly to determine its performance in improving soil shear strength.

2.2.3 | Data Analysis

Shear stress–strain curves were generated for each test specimen to evaluate the soil's response to shear loading under different reinforcement conditions. These curves were plotted by correlating shear stress with horizontal displacement for each configuration. Peak shear strength values, which represent the maximum shear stress that the soil can withstand before failure, were extracted from these curves for further analysis.

The Mohr–Coulomb failure criterion was then applied to determine the cohesion (c) and friction angle (ϕ) of the soil. This criterion describes the relationship between shear stress and normal stress at failure. The following equations were used for these calculations:

1. Shear Strength Equation: This equation relates the shear strength of the soil to the normal stress and the internal friction angle. It accounts for both the cohesion of the soil and the frictional resistance provided by the soil particles (Equation (1)).

$$\tau = c + \sigma * tan(\phi) \tag{1}$$

Whereby, τ is the shear strength, c is the cohesion, σ is the normal stress, and ϕ is the friction angle.

2. Cohesion calculation: To determine the cohesion of the soil, this equation uses the difference in shear strengths measured at two different normal stresses. It isolates the cohesion component from the overall shear strength (Equation (2)).

$$c = \frac{\tau_1 - \tau_2}{2 \times tan(\phi))} \tag{2}$$

whereby, τ_1 and τ_2 are the shear strengths at two different normal stresses, σ_1 and σ_2 are the corresponding normal stresses.

3. Friction angle calculation: This equation calculates the friction angle based on the difference in shear strengths and normal stresses at two points. It provides a measure of the soil's resistance to shear failure due to friction (Equation (3)).

$$\phi = \arctan\left(\frac{\tau_1 - \tau_2}{\sigma_1 - \sigma_2}\right) \tag{3}$$

2.2.4 | Swelling Test Data

Swelling strain: To evaluate the swelling behavior of the soil specimens, vertical displacement data obtained from the swelling tests were analyzed. The swelling strain was calculated using the following equation, which quantifies the extent of volumetric expansion relative to the initial specimen height (Equation (4)).

$$\text{Swelling Strain } (\varepsilon s) = \frac{\Delta H}{H_0} \tag{4}$$

whereby, εs is the swelling strain, ΔH is the change in height of the specimen, and H_0 is the initial height of the specimen.

Swelling potential: The swelling potential of the soil was assessed by comparing the swelling strains of the unreinforced soil to those reinforced with the biodegradable geocell and the conventional woven geogrid. A reduction in swelling strain for the reinforced specimens compared to the unreinforced specimens indicated a reduction in swelling potential.

2.3 | Comparative Performance Index (CPI)

To provide a holistic comparison of reinforcement efficiency, a dimensionless Comparative Performance Index (CPI) was developed. This metric integrates the relative improvements in cohesion (c), friction angle (φ), and peak shear strength (τ_{max}) into a single index (Equation (5)).

$$\text{CPI} = \frac{\left(\frac{C_r}{C_0} + \frac{tan\emptyset_r}{tan\emptyset_0} + \frac{\tau_{max,r}}{t_{max,0}}\right)}{3} \tag{5}$$

whereby, CPI is a dimensionless metric that integrates normalized improvements in cohesion (c), friction angle (ϕ), and peak shear strength (τ_{max}) of reinforced soil relative to unreinforced control to quantify overall reinforcement effectiveness.

3 | Results

3.1 | Material Characterization

The PSD results indicate a clear shift toward finer particles as montmorillonite clay undergoes swelling. Before swelling, larger particle sizes (10–100 μm) constitute a notable portion of the clay matrix, with the highest concentration (25%) observed at 5 μm (Figure 1a). However, as swelling progresses, the proportion of fine particles (< 5 μm) increases significantly. At constant volume, there is a slight redistribution, with finer particles (0.1–1 μm) increasing by 2%–3%, while larger particles (> 10 μm) begin to decline. After swelling, the effect becomes more pronounced; particles in the 0.1–5 μm range show the highest concentration (30% at 5 μm), while coarser fractions (20–100 μm) experience a steep reduction, with particles above 50 μm dropping to just 2% or less. This trend reflects the breakdown of larger aggregates and the separation of clay platelets, a hallmark of expansive montmorillonite clay's behavior in the presence of water. The results highlight the soil's tendency to disaggregate and disperse, increasing the proportion of finer particles, which directly impacts shear strength, permeability, and overall soil stability.

The results of the statistical analysis suggest a significant relationship between dry density and shear strength for expansive montmorillonite clay used in the study. With a mean dry density of 1.75 g/cm^3 and a mean shear strength of 41.8 kPa, the analysis reveals a variance of 0.09167 for dry density and 199.067 for shear strength, indicating some degree of variability in both parameters. The pooled variance of 99.5792 further suggests a reasonable degree of consistency in the measurements. The t-statistic of −8.9744, with a corresponding very low p-value of 2.3×10^{-8} (one-tail) and 4.6×10^{-8} (two-tail), is

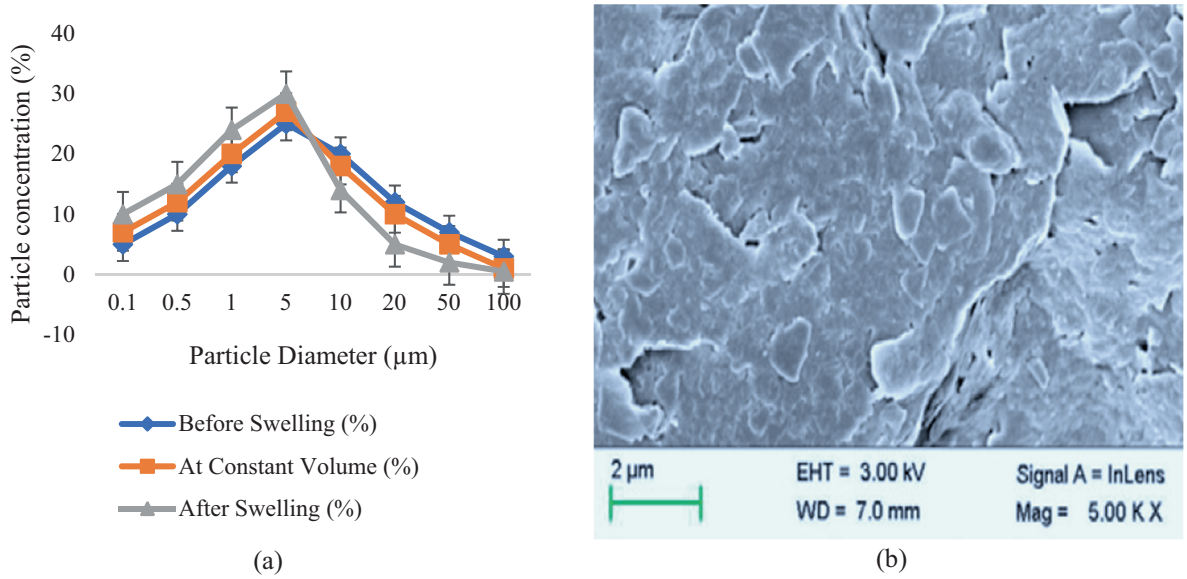

FIGURE 1 | Expansive montmorillonite clay and microstructure (a) particle size distribution (b) SEM analysis image.

TABLE 2 | Summary of the *t*-test results on dry density and shear strength.

Parameter	Dry density (g/cm^3)	Shear strength (kPa)
Mean	1.75	41.8
Variance	0.09167	199.067
Observations	10	10
Pooled variance	99.5792	
Hypothesized mean difference	0	
df	18	
t stat	−8.9744	
$P(T \leq t)$ one-tail	2.3×10^{-8}	
t critical one-tail	1.73406	
$P(T \leq t)$ two-tail	4.6×10^{-8}	
t critical two-tail	2.10092	

much smaller than the critical *t*-values of 1.73406 (one-tail) and 2.10092 (two-tail), indicating strong evidence to reject the null hypothesis. This supports the conclusion that a significant difference exists between the observed values, implying that dry density has a substantial impact on the shear strength of expansive soils (Table 2).

3.2 | Influence of Normal Stress and Reinforcement Type on Shear Strength

3.2.1 | Effect of Normal Stress on Shear Strength of Reinforced and Unreinforced Soils

The influence of normal stress on the shear strength behavior of both unreinforced and reinforced soils was systematically investigated using direct shear tests conducted at confining pressures of 50, 100, and 150 kPa. The results, illustrated in Figure 2, clearly demonstrate that shear strength increases with rising normal stress across all test conditions. This trend is consistent with classical soil mechanics theory, where higher normal stresses mobilize greater frictional resistance within the soil matrix. In the case of unreinforced soil, the peak shear strength increased from 28.1 kPa at a normal stress of 50–72.3 kPa at 150 kPa, reflecting the baseline behavior of the poorly graded sand under compression. However, the incorporation of reinforcement significantly enhanced the soil's shear resistance at each stress level. The magnitude of improvement was found to be dependent on the type of reinforcement applied. At a representative normal stress of 100 kPa, the woven geogrid-reinforced soil achieved the highest peak shear strength of 75.2 kPa, indicating a strong interlocking mechanism and tensile stiffness that effectively mobilized resistance against shearing. The nonwoven geotextile-reinforced soil followed with a peak shear strength of 63.3 kPa, benefiting primarily from surface friction and confinement effects. The biodegradable geocell-reinforced soil, while demonstrating notable enhancement over the unreinforced condition, showed a relatively modest improvement, particularly under low normal stress; for instance, at 50 kPa, it recorded a peak shear strength of 33.1 kPa compared to 28.1 kPa for the unreinforced soil. These findings confirm that both increasing confinement and the strategic use of reinforcement significantly improve the shear strength of sandy soils. Among the reinforcements tested, the woven geogrid exhibited the most effective performance, attributed to its high tensile modulus and optimal interfacial interaction with the soil particles.

3.2.2 | Time-Dependent Performance Under Varying Confinement

To assess the time-dependent behavior of reinforced soils under confinement, shear strength measurements were taken after a 1-h interval at different normal stresses, with results summarized in Figure 3. The data reveal a consistent trend: shear strength

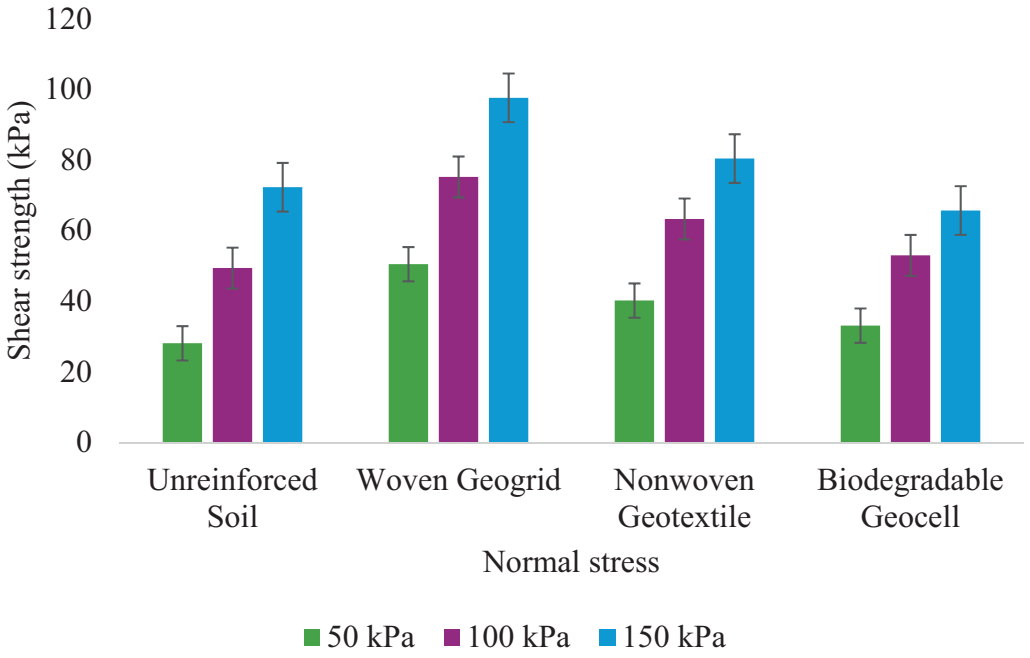

FIGURE 2 | Effect of normal stress on reinforced soil behavior.

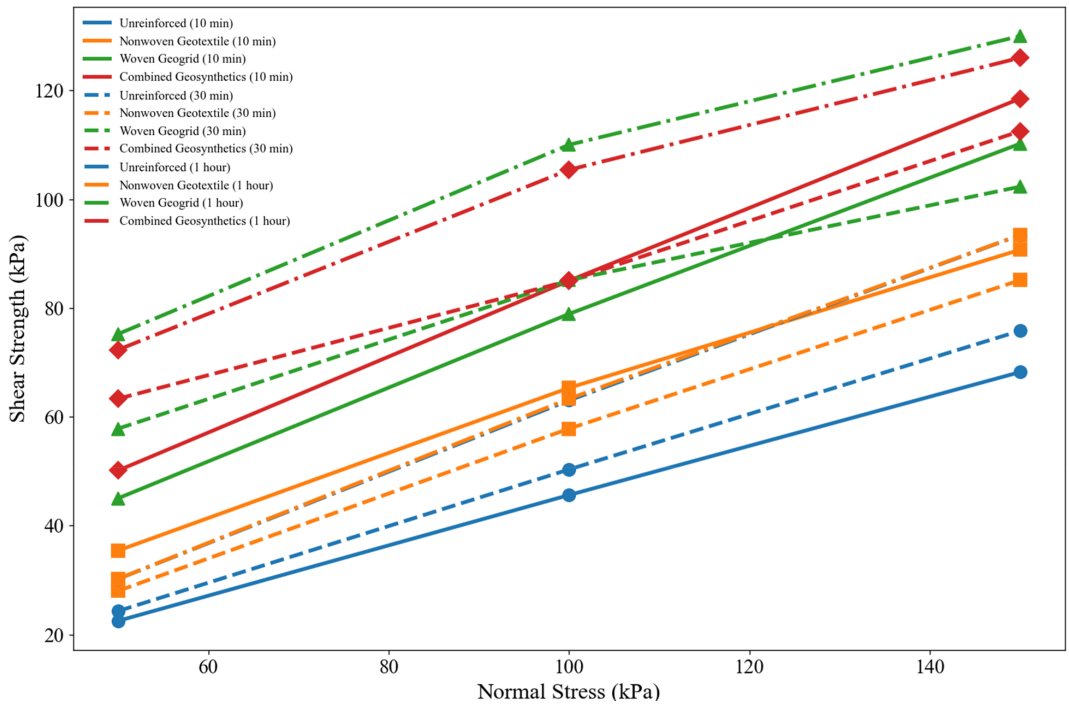

FIGURE 3 | Shear strength vs. normal stress and time-dependent performance.

increases not only with the level of confinement but also over time. This time-related gain in shear strength is more pronounced in reinforced soils, indicating the continued mobilization of tensile resistance and improved interfacial bonding between the reinforcement and the surrounding soil matrix. At a high confining pressure of 150 kPa after 1 h, the woven geogrid-reinforced soil demonstrated the most substantial improvement, achieving a peak shear strength of 130.0 kPa. This underscores the geogrid's high tensile stiffness and effective stress transfer capabilities over time. The combined geosynthetic system, comprising both woven geogrids and nonwoven geotextiles, also showed excellent performance, with a peak shear strength of 126.0 kPa. This suggests a synergistic interaction between the two reinforcement types, enhancing overall soil stability. Nonwoven geotextile-reinforced soil recorded a peak strength of 93.4 kPa under the same conditions, which was modestly higher than the corresponding value for unreinforced soil. While the exact value of the unreinforced sample may vary slightly, it consistently remained the lowest among all tested configurations. These findings highlight the superior and sustained performance of geosynthetic

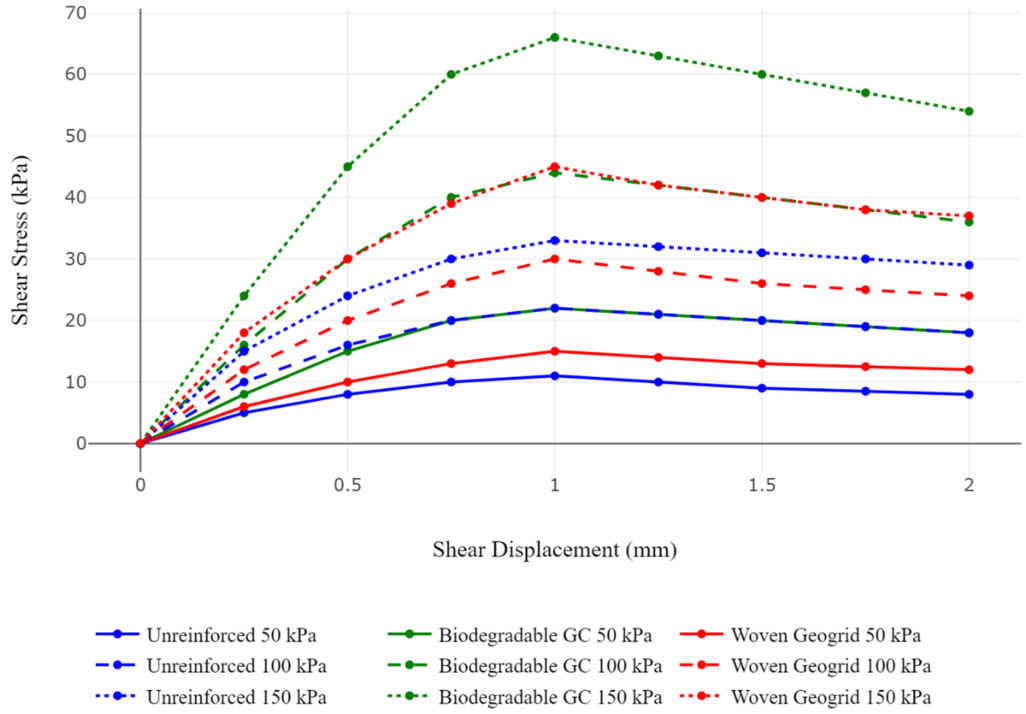

FIGURE 4 | Shear stress–strain curves for different reinforcement configurations and normal stress levels.

reinforcements, particularly woven geogrids, under elevated normal stresses and extended loading durations. The results also support the effectiveness of combined reinforcement systems, which can offer enhanced stabilization in applications demanding both immediate and long-term soil strength improvement.

3.2.3 | Influence of Reinforcement Type on Stress–Strain Behavior

The shear stress–strain response of soils under varying reinforcement types and confining pressures is illustrated in Figure 4, offering valuable insights into their deformation characteristics. Across all tests, a consistent pattern emerges: shear stress increases linearly with displacement during the initial loading phase, reaches a peak, and then gradually declines or stabilizes, indicative of strain softening or strain hardening behavior depending on the reinforcement used. Reinforced soils consistently demonstrate higher peak shear stresses compared to unreinforced specimens, along with improved ductility and enhanced resistance to deformation. The type of reinforcement significantly influences the post-peak behavior and overall stress–strain response. Biodegradable geocell-reinforced soils display superior performance at elevated confining pressures, marked by higher peak stresses and evidence of strain hardening, suggesting effective load redistribution and sustained reinforcement interaction. In contrast, woven geogrid-reinforced soils, while achieving high peak strengths, exhibit a relatively sharper decline in shear stress post-peak, indicative of more brittle failure behavior. This contrast suggests that while woven geogrids are effective in mobilizing strength quickly, biodegradable geocells offer more progressive and ductile reinforcement, making them particularly suitable for applications where long-term stability and interaction with vegetation root systems are expected to enhance performance. These findings underscore the importance of selecting reinforcement types based on the specific deformation and durability requirements of geotechnical applications.

3.3 | Influence of Reinforcement Type and Orientation on Shear Strength Parameters Under Varying Normal Stresses

The results presented in Table 3 reveal a clear distinction in the effectiveness of different reinforcement configurations on the shear strength parameters of sand under a normal stress of 50 kPa. Among all reinforcements, the combined geotextile and geogrid configuration (horizontal + perpendicular) exhibited the highest enhancement in shear strength (44.5 kPa), corresponding to a 48.3% increase relative to the unreinforced condition. This configuration also recorded the highest friction angle (39.2°, a 35.2% increase) and cohesion (18 kPa, a 125% increase), indicating strong interfacial bonding and confinement benefits when both reinforcements are synergistically oriented. The low coefficient of variation (2.3%) for this combination further reinforces the consistency and reliability of this reinforcement method. The woven geogrid in horizontal placement also showed substantial improvements, boosting shear strength by 33.3%, friction angle by 31%, and cohesion by 62.5%. These results suggest that the lateral alignment of stiff inclusions facilitates more effective stress transfer and particle interlock. Similarly, the hybrid geogrid + geocell and geotextile + geocell combinations delivered notable enhancements in shear strength (30.7% and 23.7%, respectively), although the improvements were slightly less than those achieved with geogrid-geotextile composites. In contrast, nonwoven geotextiles, regardless of placement orientation, offered only moderate performance gains (5% and 2% increases in shear strength), pointing to their lower tensile strength and limited structural contribution compared to gridded

TABLE 3 | Shear strength parameters at 50 kPa normal stress.

Reinforcement type	Orientation	Friction angle (°)	% Friction angle	Cohesion (kPa)	% Cohesion	Shear strength (kPa)	%↑Shear strength	CV (%)
Unreinforced	—	29	—	8	—	30	—	3.1
Nonwoven geotextile	Horizontal	35	20.7	15	87.5	31.5	5.	2.7
Nonwoven geotextile	Perpendicular	34	17.2	12	50	30.6	2	2.9
Woven geogrid	Horizontal	38	31	13	62.5	40	33.3	2.5
Woven geogrid	Perpendicular	36	24.1	10	25	36	20	2.6
Biodegradable geocell	Horizontal	33.6	15.9	9.2	15	22.5	−25	3.3
Biodegradable geocell	Perpendicular	31.5	8.6	8	0	20.6	−31.3	3.6
Geotextile + geogrid	Horizontal (GT) + perpendicular (GG)	39.2	35.2	18	125	44.5	48.3	2.3
Geogrid + geocell	Horizontal (GG) + perpendicular (GC)	36.8	26.9	14.5	81.3	39.2	30.7	2.5
Geotextile + geocell	Horizontal (GT) + perpendicular (GC)	35.5	22.4	13.2	65	37.1	23.7	2.6

TABLE 4 | Shear strength parameters at 100 kPa normal stress.

Reinforcement type	Orientation	Friction angle (°)	% Friction angle	Cohesion (kPa)	% Cohesion	Shear strength (kPa)	% Shear strength	CV (%)
Unreinforced	—	29	—	8	—	50	—	3
Nonwoven geotextile	Horizontal	34.7	19.7	14.8	85	63.5	27	2.8
Nonwoven geotextile	Perpendicular	33.5	15.5	12.3	53.8	61.1	22.2	2.9
Woven geogrid	Horizontal	37.6	29.7	12.9	61.3	74.7	49.4	2.4
Woven geogrid	Perpendicular	35.8	23.4	10.2	27.5	71.6	43.2	2.5
Biodegradable geocell	Horizontal	33.2	14.5	9.1	13.8	55.2	10.4	3.4
Biodegradable geocell	Perpendicular	31.4	8.3	8	0	50.7	1.4	3.6
Geotextile + geogrid	Horizontal (GT) + perpendicular (GG)	39.4	35.9	17.8	122.5%	79.4	58.8	2.3
Geogrid + geocell	Horizontal (GG) + perpendicular (GC)	37.1	27.9	13.7	71.3	73.2	46.4	2.6
Geotextile + geocell	Horizontal (GT) + perpendicular (GC)	35.6	22.8	13.4	67.5	66.5	33	2.7

or cellular reinforcements. Notably, biodegradable geocells, both in horizontal and perpendicular placement, showed poor performance, with negative improvements in shear strength (−25% and −31.3%, respectively). Although they slightly improved the friction angle and marginally increased cohesion in the horizontal configuration, these gains were insufficient to offset the reduction in overall shear strength. This trend highlights the limitations of biodegradable geocells under normal loading conditions, possibly due to their relatively low stiffness and susceptibility to deformation. Overall, placement effectiveness was closely aligned with reinforcement type and configuration, with combinations offering synergistic orientations outperforming single-material systems and confirming the value of integrated reinforcement strategies in sandy soil stabilization.

The results summarized in Table 4 indicate that under normal stress of 100 kPa, reinforced sand specimens exhibit notable improvements in shear strength parameters compared to the unreinforced baseline. Among the tested reinforcements, the combined geotextile and geogrid system (horizontal GT + perpendicular GG) again demonstrated the highest performance, yielding the greatest increase in shear strength (79.4 kPa; 58.8% improvement), the highest friction angle (39.4°, +35.9%), and the highest cohesion (17.8 kPa; +122.5%). This configuration also maintained a low coefficient of variation (2.3%), indicating high consistency in shear behavior under elevated normal stress. The woven geogrid (horizontal) followed closely, producing a 49.4% increase in shear strength and substantial increases in both friction angle (+29.7%) and cohesion (+61.3%). Its perpendicular placement was also effective, though slightly less so. These results highlight the efficient interlocking and tensile resistance offered by woven geogrids, especially when oriented to resist lateral displacement. Hybrid systems, including geogrid + geocell and geotextile + geocell, provided marked enhancements in shear strength (46.4% and 33.0%, respectively), reinforcing the benefit of integrating cellular and planar reinforcements. However, their performance was moderately lower than that of the geogrid–geotextile composite. Notably, nonwoven geotextiles, whether placed horizontally or perpendicularly, delivered moderate gains in shear strength (27.0% and 22.2%), consistent with their flexible structure and relatively lower tensile capacity. In contrast, biodegradable geocells showed

TABLE 5 | Shear strength parameters at 150 kPa normal stress.

Reinforcement type	Orientation	Friction angle (°)	% Friction angle	Cohesion (kPa)	% Cohesion	Shear strength (kPa)	% Shear strength	CV (%)
Unreinforced	—	29	—	8	—	75	—	3.2
Nonwoven geotextile	Horizontal	34.9	20.3	14.9	86.3	95.3	27.1	2.9
Nonwoven geotextile	Perpendicular	33.6	15.9	12.1	51.3	91.1	21.5	3.1
Woven geogrid	Horizontal	37.7	30	13.2	65	110.2	46.9	2.5
Woven geogrid	Perpendicular	35.9	23.8	10.3	28.8	107.7	43.6	2.6
Biodegradable geocell	Horizontal	33.3	14.8	9	12.5	82.2	9.6	3.5
Biodegradable geocell	Perpendicular	31.4	8.3	8	0	76.1	1.5	3.7
Geotextile + geogrid	Horizontal (GT) + perpendicular (GG)	39.6	36.6	17.6	120	115.8	54.4	2.4
Geogrid + geocell	Horizontal (GG) + perpendicular (GC)	37.2	28.3	13.5	68.8	108.9	45.2	2.7
Geotextile + geocell	Horizontal (GT) + perpendicular (GC)	35.8	23.4	13.3	66.3	98.1	30.8	2.9

TABLE 6 | Impact of reinforcement position on shear strength and cohesion at 50 kPa normal stress.

Reinforcement position	Material type	Shear strength (kPa)	Cohesion (kPa)
Mid-height (horizontal)	Nonwoven geotextile	51.2	15
Mid-height (horizontal)	Woven geogrid	65.5	9.9
Mid-height (horizontal)	Biodegradable geocell	48.7	11.3
Different configurations	Geosynthetic (combined)	68.5	17.9

minimal improvement in shear strength: 10.4% for horizontal placement and a mere 1.4% for perpendicular orientation. The friction angle and cohesion gains were also marginal to negligible in this group, suggesting that biodegradable geocells may be inadequate under higher normal stress conditions due to potential deformation or limited stiffness. Generally, the ranking of placement effectiveness closely follows the trends observed at 50 kPa, affirming the superior performance of composite and stiff reinforcements and the critical role of proper orientation in mobilizing shear resistance in sandy soils. The clear hierarchy, composite > woven geogrid > hybrid with geocell > nonwoven geotextile > biodegradable geocell, reinforces the value of both material selection and structural integration in soil reinforcement applications under increased loading conditions.

The results presented in Table 5 under normal stress of 150 kPa reaffirm the shear strength enhancement trends observed at lower stress levels, with composite and stiff reinforcements exhibiting the most pronounced improvements. The horizontal geotextile + perpendicular geogrid system again outperformed all other configurations, showing a 54.4% increase in shear strength (to 115.8 kPa), a 36.6% rise in friction angle, and a 120% gain in cohesion. Its low coefficient of variation (2.4%) highlights consistent performance under elevated loading, reinforcing its designation as the most effective placement. Following this, the horizontal woven geogrid produced a 46.9% shear strength gain, supported by a significant rise in friction angle (+30.0%) and cohesion (+65.0%). Its perpendicular configuration also remained effective, confirming that geogrids, owing to their tensile stiffness and interlocking action, are reliable even when oriented against the direction of shear mobilization. Hybrid reinforcements also performed well: the geogrid + geocell combination resulted in a 45.2% increase in shear strength, while the geotextile + geocell system achieved a 30.8% gain. These results validate the synergistic benefits of combining cellular and planar reinforcements, especially under high confining pressures. Nonwoven geotextiles, though lower in tensile capacity, still delivered respectable shear strength enhancements (27.1% for horizontal, 21.5% for perpendicular), with significant cohesion improvements. Their moderate variability and ease of placement make them suitable for moderate loading scenarios. In contrast, biodegradable geocells again provided minimal improvement, especially in perpendicular orientation (+1.5% in shear strength, 0% in cohesion). These results suggest structural degradation or limited confinement capacity under 150 kPa, limiting their utility under such stress conditions. In summary, the ranking under 150 kPa stress reinforces previous trends: Composite (GT + GG) > Woven Geogrid > Hybrid (GG + GC or GT + GC) > Nonwoven Geotextile > Biodegradable Geocell.

3.4 | Reinforcement Response to Mid-Height Position

Table 6 presents the impact of different reinforcement materials on soil shear strength and cohesion when placed at the mid-height (horizontal) position or using different configurations. The data show that the type of reinforcement material significantly affects both the shear strength and cohesion of the

TABLE 7 | Impact of reinforcement position on shear strength and cohesion at 100 kPa normal stress.

Reinforcement position	Material type	Shear strength (kPa)	Cohesion (kPa)
Mid-height (horizontal)	Nonwoven geotextile	61.4	15
Mid-height (horizontal)	Woven geogrid	78.6	10.5
Mid-height (horizontal)	Biodegradable geocell	58.4	12
Different configurations	Geosynthetic (combined)	82.2	18.5

TABLE 8 | Impact of reinforcement position on shear strength and cohesion at 150 kPa normal stress.

Reinforcement position	Material type	Shear strength (kPa)	Cohesion (kPa)
Mid-height (horizontal)	Nonwoven geotextile	69.8	15
Mid-height (horizontal)	Woven geogrid	91.2	11
Mid-height (horizontal)	Biodegradable geocell	66	12.5
Different configurations	Geosynthetic (combined)	94.5	19

soil. Nonwoven geotextile, woven geogrid, and biodegradable geocell, each placed horizontally in the mid-height position, demonstrate varying impacts on these soil properties. Additionally, the table provides results for a combination of geosynthetics, illustrating how different reinforcement strategies can interact to enhance soil performance. The shear strength values for the different materials range from 48.7 kPa for the biodegradable geocell to 68.5 kPa for the combined geosynthetics. The woven geogrid exhibits the highest shear strength, indicating that it might provide the most effective reinforcement in terms of increasing the soil's resistance to shear failure. Conversely, the biodegradable geocell, while contributing to shear strength, shows a lower value compared to the woven geogrid and combined geosynthetics, suggesting that it might be less effective in improving soil shear strength. In terms of cohesion, the results also vary among the materials. The nonwoven geotextile and the combined geosynthetics provide higher cohesion values (15 and 17.9 kPa, respectively) compared to the woven geogrid (9.9 kPa) and biodegradable geocell (11.3 kPa). Higher cohesion values generally reflect better soil bonding and stability, which is crucial for ensuring the overall stability and performance of the reinforced soil. These variations highlight how different materials not only influence shear strength but also affect the soil's inherent cohesion, thereby impacting the overall effectiveness of the reinforcement strategies.

Table 7 illustrates the effect of various reinforcement materials on soil shear strength and cohesion when positioned horizontally at mid-height or using different configurations. The results highlight that different reinforcement types significantly impact the soil's shear strength and cohesion, which are crucial for assessing the effectiveness of soil stabilization techniques. The materials tested include nonwoven geotextile, woven geogrid, biodegradable geocell, and a combination of geosynthetics, providing insights into how each influences soil properties. The shear strength values in the table range from 58.4 kPa for the biodegradable geocell to 82.2 kPa for the combined geosynthetics. The woven geogrid shows the highest shear strength, indicating that it may be the most effective reinforcement in enhancing the soil's resistance to shear failure. The combined geosynthetics also perform well, providing a significant improvement in shear strength compared to the nonwoven geotextile and biodegradable geocell. This suggests that integrating different types of geosynthetics can further enhance soil stability and performance. Cohesion values vary among the materials, with the combined geosynthetics achieving the highest cohesion of 18.5 kPa, indicating superior soil bonding and stability. The nonwoven geotextile provides a moderate cohesion value of 15 kPa, while the woven geogrid and biodegradable geocell show lower cohesion values of 10.5 and 12 kPa, respectively. These results underscore that while shear strength is significantly improved by various reinforcements, cohesion, which contributes to soil stability and performance, also benefits from specific reinforcement strategies.

Table 8 provides the impact of different reinforcement materials on soil shear strength and cohesion under normal stress of 150 kPa. The data presented helps in understanding how various types of reinforcements influence soil behavior under higher loading conditions, which is crucial for practical applications in geotechnical engineering. At this normal stress level, the shear strength values have increased compared to those at lower stress levels, reflecting the soil's enhanced resistance to shear failure under increased load. The woven geogrid exhibits the highest shear strength of 91.2 kPa, indicating its superior performance in strengthening the soil. The combined geosynthetics also show a significant shear strength of 94.5 kPa, suggesting that combining different geosynthetics can further enhance the soil's stability. In terms of cohesion, the combined geosynthetics provide the highest value of 19 kPa, demonstrating improved soil bonding and stability compared to the other materials. The nonwoven geotextile maintains a constant cohesion of 15 kPa, while the woven geogrid and biodegradable geocell have lower cohesion values of 11 and 12.5 kPa, respectively. This highlights that while the shear strength benefits from various reinforcement types, cohesion improvements vary, with the combined geosynthetics offering the most significant enhancement in soil stability.

3.5 | Swelling Behavior

The swelling strain results for both reinforced and unreinforced soils across different normal stresses (50, 100, and 150 kPa) reveal distinct patterns that highlight the effectiveness of the

TABLE 9 | Swelling strain of the reinforced and unreinforced soil.

	Swelling strain (%)		
Reinforcement	**50 kPa**	**100 kPa**	**150 kPa**
Unreinforced	12.8	10.2	8.5
Biodegradable GC	4.2	3.8	3.1
Woven geogrid	7.5	6.4	5.8

TABLE 10 | Comparative performance index (CPI) of reinforcement configurations.

Reinforcement type	Orientation/placement	CPI	CPI rating
Biodegradable geocell	Vertical	1.81	High
Woven geogrid	Dual-horizontal	1.75	High
Woven geogrid	Horizontal	1.62	Moderate to high
Geotextile + geogrid	Horizontal (GT) + perpendicular (GG)	1.58	Moderate to high
Nonwoven geotextile	Horizontal	1.42	Moderate
Geotextile + geocell	Horizontal (GT) + perpendicular (GC)	1.37	Moderate
Nonwoven geotextile	Perpendicular	1.32	Moderate
Woven geogrid	Perpendicular	1.27	Moderate
Biodegradable geocell	Horizontal	1.18	Low to moderate
Biodegradable geocell	Perpendicular	1.08	Low
Unreinforced	—	1	Baseline

reinforcements used. At 50 kPa, the unreinforced soil exhibits the highest swelling strain of 12.8%, indicating significant volume expansion due to moisture absorption. This high swelling strain is reduced considerably when reinforcements are applied, with the biodegradable geocell (GC) showing the lowest swelling strain at 4.2%, and the woven geogrid showing a moderate reduction with a swelling strain of 7.5%. These results suggest that the reinforcements, particularly the biodegradable geocell, are effective in mitigating the swelling potential of the soil under low normal stress. As the normal stress increases to 100 kPa, there is a noticeable decrease in swelling strain across all samples, which is consistent with the general behavior of soils under higher compressive loads. The unreinforced soil's swelling strain decreases to 10.2%, while the biodegradable geocell and woven geogrid reduce swelling strain further to 3.8% and 6.4%, respectively. The continued lower swelling strain in reinforced soils indicates that the reinforcements provide structural stability, reducing the soil's tendency to swell even under moderate stress. This suggests that the reinforcements are helping to confine the soil particles, limiting their movement and, consequently, their ability to absorb water and swell. At the highest normal stress level of 150 kPa, the trend of decreasing swelling strain continues, with the unreinforced soil showing a strain of 8.5%, while the biodegradable geocell and woven geogrid exhibit swelling strains of 3.1% and 5.8%, respectively. The effectiveness of the reinforcements becomes even more apparent under this high-stress condition, as they significantly reduce the soil's swelling potential compared to the unreinforced sample. The biodegradable geocell, in particular, continues to demonstrate superior performance in limiting swelling strain, which could be attributed to its ability to provide greater confinement and stability to the soil matrix. Overall, these results demonstrate that the use of geosynthetic reinforcements, especially the biodegradable geocell, significantly reduces swelling strain in soils under varying normal stresses. The reduction in swelling strain with increasing normal stress further emphasizes the stabilizing effect of these reinforcements, making them suitable for use in conditions where soil swelling could lead to instability or structural damage. The data also suggest that biodegradable options like the geocell not only provide effective reinforcement but also offer environmental benefits, making them an attractive option for sustainable engineering applications (Table 9).

3.6 | Statistical Analysis

3.6.1 | Comparative Performance Index (CPI)

The Comparative Performance Index (CPI) results presented in Table 10 highlight the significant influence of reinforcement type and placement orientation on the mechanical performance of poorly graded sand. The highest CPI of 1.81 was observed for the biodegradable geocell placed vertically, indicating superior performance due to the optimal confinement and stress distribution it provides through its cellular structure. This was closely followed by the dual-horizontal configuration of the woven geogrid (CPI = 1.75), which benefits from enhanced lateral confinement and interlocking efficiency in two planes. The horizontal placement of the woven geogrid alone also showed strong performance (CPI = 1.62), outperforming more complex hybrid configurations, such as geotextile plus geogrid (1.58) and geotextile plus geocell (1.37), which may have suffered from partial interaction or reinforcement interference effects. Nonwoven geotextiles in horizontal and perpendicular placements yielded moderate CPI values (1.42 and 1.32, respectively), reflecting their limited tensile stiffness and ability to redistribute stresses effectively. The

TABLE 11 | Summary of the ANOVA results.

Source of variation	SS	df	MS	F	p	F crit
Between groups	32 132.3	2	16 066.15	215.54	1.01×10^{-14}	3.4668
Within groups	1565.33	21	74.54			
Total	33 697.63	23				

TABLE 12 | Post hoc analysis: Tukey HSD.

Comparison	Mean difference	p	Significant ($p < 0.01$)
Biodegradable geocell (vertical) vs. nonwoven geotextile (horizontal)	23.44	1.27×10^{-6}	Yes
Biodegradable geocell (vertical) vs. geotextile + geocell (H + P)	63.2	1.09×10^{-8}	Yes
Nonwoven geotextile (horizontal) vs. geotextile + geocell (H + P)	86.64	9.33×10^{-9}	Yes

lowest performances were recorded for the biodegradable geocell placed horizontally (1.18) and perpendicularly (1.08), both of which likely failed to provide adequate confinement due to the orientation of the cells relative to the loading direction. The unreinforced case, set as the baseline with a CPI of 1.00, clearly underscores the enhancement provided by reinforcement strategies, with vertical and dual-horizontal configurations proving the most effective for improving the soil's load-bearing capacity.

3.6.2 | Analysis of Variance (ANOVA)

The Analysis of Variance (ANOVA) results presented in Table 11 provide a robust statistical validation of the observed differences in Comparative Performance Index (CPI) values among different reinforcement configurations. The F-value of 215.54, which is significantly greater than the critical F-value (F crit = 3.4668) at the 95% confidence level, strongly indicates that there are statistically significant differences in CPI among the tested reinforcement groups. Furthermore, the extremely low p-value (1.01×10^{-14}), which is far below the typical significance threshold of 0.05, confirms that these differences are not due to random chance. The large sum of squares between groups (SS = 32132.3) compared to the sum of squares within groups (SS = 1565.33) also reflects the substantial variation accounted for by the type and placement of reinforcement, rather than experimental error. This analysis reinforces the conclusion that reinforcement configuration has a significant effect on the mechanical performance of the soil and justifies further optimization based on CPI outcomes.

3.6.3 | Tukey Honestly Significant Difference

The results of the Tukey Honestly Significant Difference (HSD) post hoc analysis provide clear insights into the specific pairwise differences in performance between reinforcement configurations following the ANOVA. All three comparisons yielded statistically significant differences at the $p < 0.01$ level, affirming that the variations in the Comparative Performance Index (CPI) observed are not only statistically significant overall but also meaningfully distinct between specific reinforcement pairs. The biodegradable geocell placed vertically demonstrated a mean CPI difference of 23.44 compared to the nonwoven geotextile in horizontal orientation, with a p-value of 1.27×10^{-6}, confirming its superior performance. Moreover, the same vertical geocell configuration outperformed the combined geotextile and geocell system (horizontal + perpendicular) by a substantial margin of 63.2, with an even more significant p-value of 1.09×10^{-8}. Notably, even between two moderately performing configurations—nonwoven geotextile (horizontal) and geotextile + geocell (H + P), a significant difference of 86.64 was observed ($p = 9.33 \times 10^{-9}$), emphasizing the sensitivity of soil reinforcement performance to both material type and placement orientation. These findings underscore the importance of carefully selecting and configuring reinforcement systems to maximize soil stabilization effectiveness (Table 12).

3.7 | Physical Model Tests

To validate the findings obtained from small-scale direct shear tests, a series of physical model tests were conducted using a large soil tank ($1.2 \times 1.0 \times 0.8$ m) to simulate field-like conditions. The models comprised unreinforced and reinforced expansive clay beds subjected to surface loading through a rigid circular footing of 150 mm diameter. Reinforcement configurations included: (a) single-layer nonwoven geotextile (PP), (b) single-layer woven geogrid (TX140), (c) biodegradable geocell, and (d) combined geocell–geogrid system. The load–settlement behavior and failure patterns were analyzed to assess reinforcement performance. The results presented in Figure 5 demonstrate a clear enhancement in load–settlement behavior of expansive clay when reinforced with various geosynthetic configurations. The unreinforced clay model exhibited the lowest peak bearing capacity (42 kPa) with significant settlement. Introducing a nonwoven geotextile increased the bearing capacity by 52.4% and reduced settlement by 28%, while the woven geogrid showed slightly better performance with a 64.3% increase in bearing capacity and a 34% reduction in settlement. The biodegradable geocell provided even greater improvements, boosting bearing capacity by 85.7% and cutting settlement by 46%. The most effective configuration was the combined geocell–geogrid system, which yielded the highest bearing capacity (96 kPa), representing a 128.5% increase over the unreinforced case, and reduced settlement by 60%, indicating superior load distribution and confinement capabilities under surface loading.

4 | Discussion

The experimental findings confirm that normal stress plays a pivotal role in influencing the shear strength of both reinforced

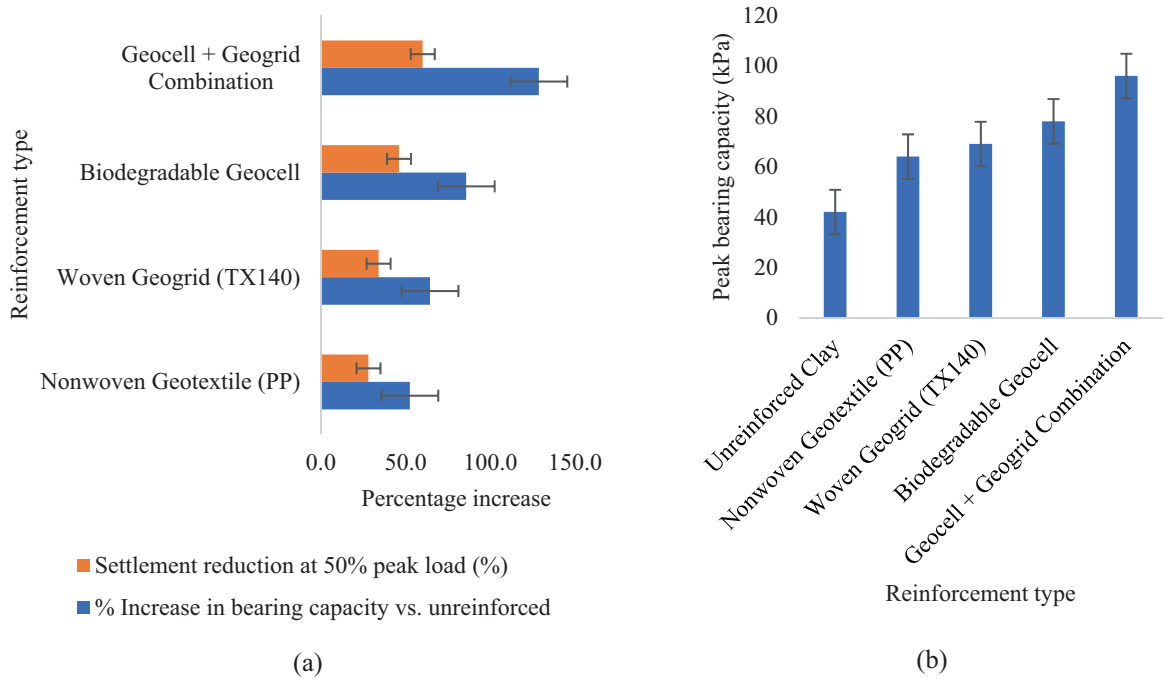

FIGURE 5 | Load–settlement behavior (a) % Increase in bearing capacity vs. unreinforced and settlement reduction at 50% peak load (%) (b) peak bearing capacity.

and unreinforced soils, aligning well with the Mohr-Coulomb failure criterion. As the applied normal stress increased, shear strength improved across all configurations due to enhanced frictional resistance and better mobilization of reinforcement. This trend was especially evident in soils reinforced with woven geogrids, which exhibited peak shear strengths exceeding 40 kPa under high normal stress, attributable to their high tensile stiffness and efficient soil-interlocking capabilities. These properties enable geogrids to distribute shear loads effectively across the soil mass, minimizing deformation and increasing resistance to failure. Similar reinforcement mechanisms were observed in the study by Azzam and Basha [19], who found that incorporating vertical steel inclusions in cohesive soils significantly increased shear strength by up to 231% while also reducing settlement. Their results emphasized that vertical elements not only share applied loads with the surrounding soil but also alter the failure mechanism from brittle to more ductile modes, which parallels the observed behavior of stiff reinforcements like geogrids. Conversely, the performance of biodegradable geocells under varying normal stress was more modest, with peak shear strength gains limited to about 15%–20%, likely due to their relatively lower stiffness and reduced interfacial friction, which limited their engagement with the surrounding soil. According to Zhao et al. [20], such limited improvement in geocell-reinforced cohesive beds can be attributed to the low modulus and cohesion of the infill material, which impairs the ability of the geocell to mobilize reinforcement. Their parametric simulations suggest that geocell performance is markedly enhanced when filled with higher-modulus, lower-cohesion soils, emphasizing the importance of matching reinforcement type and infill properties to the mechanical demands of a given application. Overall, the findings suggest that geosynthetic selection should be carefully aligned with anticipated loading and soil conditions to maximize reinforcement effectiveness.

Time-dependent performance analysis revealed that reinforced soils, especially those incorporating woven geogrids, exhibited substantial improvements in shear strength over extended durations, notably under higher confining pressures. This enhancement is attributed to the continuous mobilization of tensile forces within the reinforcement layers and the progressive stress redistribution at the soil-reinforcement interface, leading to improved interfacial bonding over time. The observed long-term gains align with findings by Yang et al. [21], who demonstrated that geogrid-reinforced expansive soils transitioned from strain-softening to strain-hardening behavior with increasing reinforcement layers and freeze–thaw cycles, further emphasizing the durability of geogrid-reinforced systems under cyclic environmental stress. The superior performance of combined reinforcement systems likely results from the synergistic interaction of distinct reinforcement mechanisms; nonwoven geotextiles provide interfacial bonding and filtration, while woven geogrids and geocells contribute tensile stiffness and lateral confinement. This is consistent with the conclusions of Hassan et al. [22], who reported that geotextiles, due to higher interface friction and tensile strength, yielded up to 241% improvement in shear strength in non-plastic cohesive soils compared to 140% with geogrids, highlighting material-dependent interaction behavior. Furthermore, large-scale triaxial tests conducted by Chen et al. [23] on weathered mudstone-based coarse-grained soils revealed that shear deformation exhibited strain-hardening behavior with increased confining pressure and geogrid layers. This behavior was linked to improved apparent cohesion and gradual dissipation of pore water pressure during shearing, supporting the long-term stabilization potential of reinforced fills. Collectively, these studies corroborate the effectiveness of hybrid geosynthetic reinforcement systems in sustaining load resistance and enhancing long-term stability, making them highly suitable for critical

infrastructure applications such as embankments, reinforced soil slopes, and retaining walls.

The stress–strain behavior of reinforced soils offers critical insights into their mechanical responses under shear loading conditions. Reinforced specimens consistently exhibited higher peak shear strengths and more ductile failure patterns than their unreinforced counterparts, indicating enhanced energy absorption and resistance to deformation. This behavior aligns with the results reported by Botero et al. [24], who observed that silty soils reinforced with discrete polyethylene terephthalate (PET) fibers showed increased shear strength and deformation capacity, enhancing their suitability for geotechnical structures that demand high ductility, such as landfills and containment systems. Similarly, Evangelou et al. [25], found that the use of polypropylene fibers in soils led to a transition from brittle to ductile behavior, with substantial increases in cohesion (up to sevenfold) and relatively moderate changes in the internal friction angle (±25%). The type and structure of reinforcement played a pivotal role in defining the mechanical response. Woven geogrids enabled the rapid mobilization of shear resistance due to their rigid configuration and strong soil interlock, resulting in a sharp peak strength followed by moderate post-peak softening. In contrast, biodegradable geocells exhibited a smoother and more gradual stress–strain response, indicative of a progressive load transfer mechanism and better deformation compatibility. These distinctions are consistent with the findings of Evangelou et al. [25], where longer fibers and higher contents contributed to enhanced ductility and cohesion, especially in soils with low inherent cohesion. Furthermore, the orientation and combination of reinforcement materials were found to critically influence shear strength behavior. Configurations involving horizontal nonwoven geotextiles combined with perpendicular geogrids produced the highest gains in both apparent cohesion and internal friction angle. This can be attributed to improved confinement and interfacial friction due to the geogrid's anchorage and the geotextile's bonding capacity, which effectively restricted lateral displacement and promoted stress redistribution [26]. Conversely, horizontal placement of nonwoven geotextiles or geocells alone offered only moderate performance gains, likely due to their relatively lower structural integrity and interface friction.

When reinforcement was applied at mid-height within the soil specimen, its impact on shear strength and cohesion varied significantly depending on the material used, a trend consistent with findings from recent triaxial and numerical studies. The woven geogrid consistently outperformed other reinforcements, exhibiting superior mechanical interlock and stiffness that enhanced soil stability by anchoring particles and resisting shear-induced displacement, leading to a marked increase in cohesion. These effects align with results from Xi Wang et al. [27], where triaxial tests and discrete element simulations demonstrated that increasing geogrid layers enhanced peak strength and cohesion, while maintaining a relatively unchanged internal friction angle. The underlying mechanism was attributed to increased particle contact and coordination, reduced porosity fluctuations, and improved distribution of contact stress, all contributing to a denser, more restrained soil structure. Similarly, large-scale triaxial tests on gravelly soils by Liu et al. [28], confirmed that geogrid reinforcement significantly improved shear strength and structural integrity by limiting lateral deformation and enhancing particle confinement, even as internal friction angle remained stable. In contrast, biodegradable geocells at mid-height were less effective due to insufficient confinement and weaker soil-reinforcement interaction along the shear plane [29]. However, hybrid systems that combined geotextiles and geogrids exhibited the greatest cohesion improvements, validating the synergistic advantage of integrating materials that offer both tensile strength and surface bonding. These findings collectively reinforce the importance of reinforcement configuration, material type, and the scale of interaction in optimizing shear resistance and deformation control in reinforced soils.

Swelling behavior measurements provided compelling evidence for the efficacy of soil reinforcements in mitigating volumetric instability under moisture ingress. Among the tested materials, the biodegradable geocell exhibited superior performance in reducing swelling strain, attributed to its closed, flexible cellular architecture that offered lateral confinement and restricted particle displacement. This structural characteristic effectively limited soil expansion and preserved matrix integrity under varying stress conditions. An inverse relationship between normal stress and swelling potential was observed, underscoring the synergistic effect of external compressive forces and internal reinforcement in controlling volumetric changes [30]. These findings are particularly significant for expansive soils, where uncontrolled swelling poses substantial risks to structural durability. The superior performance of geocells highlights their potential as sustainable geotechnical solutions for enhancing volumetric stability in moisture-sensitive environments. Statistical analyses robustly supported these observations. The Comparative Performance Index (CPI) ranked vertical placements of biodegradable geocells and the dual-horizontal configuration of woven geogrids as the most effective in enhancing shear resistance and limiting swelling. High CPI values reflected improved confinement and optimal tensile mobilization, affirming the practical superiority of these configurations. ANOVA results revealed statistically significant differences across reinforcement strategies, with p-values indicating a low likelihood of random variation. Post hoc Tukey HSD tests identified the vertical biodegradable geocell arrangement as significantly outperforming both horizontal nonwoven geotextiles and combined geotextile-geocell systems. These results emphasize the influence of material type and configuration on reinforcement performance, underscoring the necessity for site-specific designs underpinned by experimental validation and rigorous statistical evaluation. These findings align with recent literature emphasizing sustainable and multifunctional approaches to soil stabilization. For example, Utkarsh and Jain [31] demonstrated the effectiveness of combined stabilizers such as expanded polystyrene (EPS), lime, and fly ash in mitigating expansive soil behavior, noting that EPS mitigates swelling through mechanical cushioning while lime and fly ash contribute through cation exchange and pozzolanic reactions. While chemical stabilizers remain prevalent, the current study's use of biodegradable geocells offers a low-impact, mechanical alternative that addresses environmental and durability concerns. Similarly, the study by Namburu et al. [32] explored geocoir cell mattresses filled with coconut shell infill, achieving a 4.98-fold increase in load-bearing capacity and an 88% reduction in settlement. These results parallel the current findings, reinforcing the

efficacy of bio-based reinforcement in enhancing geotechnical performance while promoting sustainability.

5 | Conclusion

This study investigated the effectiveness of nonwoven geotextiles and woven geogrids in enhancing the shear strength of expansive montmorillonite clay, also examining the potential of biodegradable geocells in mitigating swelling. Results conclusively demonstrate that reinforcing the expansive montmorillonite clay with either nonwoven geotextiles or woven geogrids significantly enhances its shear strength under various normal stress levels. For instance, at a normal stress of 100 kPa, geogrid reinforcement increased the shear strength from 50 kPa (unreinforced) to 65.5 kPa, while nonwoven geotextiles resulted in a shear strength of 51.2 kPa, highlighting the superior performance of geogrids in enhancing soil stability. This improvement was observed across all tested normal stress levels (50, 100, and 150 kPa), with geogrids consistently exhibiting higher shear strength values compared to nonwoven geotextiles. Additionally, the use of nonwoven geotextiles was found to increase the cohesion of the expansive montmorillonite clay from 8 to 15 kPa. Furthermore, biodegradable geocells proved highly effective in controlling swelling, reducing swelling strain from 12.8% (unreinforced) to 4.2%. This reinforcement type also consistently exhibited the highest peak shear strength and cohesion values across all tested normal stresses. For example, at 50 kPa normal stress, biodegradable geocells achieved a peak shear strength of 22.5 kPa and cohesion of 9.2 kPa, surpassing the performance of both woven geogrids (15.8 kPa shear strength, 6.1 kPa cohesion) and unreinforced soil (11.2 kPa shear strength, 3.5 kPa cohesion). Interestingly, while the reinforcement types significantly influenced shear strength and cohesion, the friction angle remained relatively consistent across different reinforcement types and normal stresses, indicating that the reinforcements primarily enhance soil strength by increasing interlocking and interaction between soil particles. This research provides a comprehensive understanding of how different geosynthetics interact with soil, offering valuable insights for optimizing ground improvement techniques. This study, while offering valuable insights through small-scale direct shear tests, is limited by the constrained box dimensions ($6 \times 6 \times 2$ cm), which may not fully replicate field stress conditions, deformation patterns, or reinforcement–soil interactions. The scale effect, boundary constraints, and simplified loading conditions can influence the mobilization of shear strength and reinforcement mechanisms, potentially limiting the generalizability of the findings. Additionally, long-term performance aspects, such as the degradation of biodegradable geocells and soil–reinforcement behavior under cyclic environmental conditions, remain unaddressed. Therefore, future research should incorporate field-scale validations to more accurately assess reinforcement effectiveness and guide practical geotechnical design.

Author Contributions

Assel Tulebekova: conceptualization, methodology, investigation, funding acquisition, writing – original draft. **Zhanar Kusbergenova:** investigation, resources. **Aliya Aldungarova:** investigation, resources. **Gulshat Tleulenova:** investigation, resources. **Dauren Yessentay:** investigation, resources. **Uliya Abdikerova:** investigation, resources. **Nargul Saktaganova:** investigation, resources. **Atogali Jumabayev:** investigation, resources. **Timoth Mkilima:** investigation, writing – original draft, writing – review and editing, methodology.

Acknowledgments

The authors would like to express their gratitude to the "ENU–Lab" laboratory complex of L.N. Gumilyov Eurasian National University for the opportunity to conduct the tests and to the director of "ENU–Lab".

Conflicts of Interest

The authors declare no conflicts of interest.

Data Availability Statement

The data that support the findings of this study are available from the corresponding author upon reasonable request.

References

1. A. A. A. Shehata, A. O. Owino, M. Y. Islam, and Z. Hossain, "Shear Strength of Soil by Using Rice Husk Ash Waste for Sustainable Ground Improvement," *Discover Sustainability* 5 (2024): 64, https://doi.org/10.1007/s43621-024-00238-x.

2. L. Igosheva and A. Grishina, "Review of the Basic Methods of the Ground Improvement," *PNRPU Construction and Architecture Bulletin* 7 (2016): 5–21, https://doi.org/10.15593/2224-9826/2016.2.01.

3. M. Ayeldeen, A. Negm, M. El-Sawwaf, and M. Kitazume, "Enhancing Mechanical Behaviors of Collapsible Soil Using Two Biopolymers," *Journal of Rock Mechanics and Geotechnical Engineering* 9 (2017): 329–339, https://doi.org/10.1016/j.jrmge.2016.11.007.

4. S. M. Haeri, A. A. Garakani, A. Khosravi, and C. L. Meehan, "Assessing the Hydro-Mechanical Behavior of Collapsible Soils Using a Modified Triaxial Test Device," *Geotechnical Testing Journal* 37 (2014): 190–204, https://doi.org/10.1520/GTJ20130034.

5. T. Mkilima, Y. Sabitov, Z. Shakhmov, et al., "Exploring the Synergistic Effect of Recycled Glass Fibres and Agricultural Waste Ash on Concrete Strength and Environmental Sustainability," *Cleaner Engineering and Technology* 20 (2024): 100752, https://doi.org/10.1016/j.clet.2024.100752.

6. G. Das and P. Ghosh, "Large-Scale Experimental and ANN Modeling for Dynamic Interaction Between Vibrating and Statically Loaded Foundations on Geogrid-Reinforced Soil Beds," *Geotextiles and Geomembranes* 52 (2024): 956–974, https://doi.org/10.1016/j.geotexmem.2024.06.001.

7. P. S. Reddy, B. Mohanty, and B. H. Rao, "Influence of Clay Content and Montmorillonite Content on Swelling Behavior of Expansive Soils," *International Journal of Geosynthetics and Ground Engineering* 6 (2020): 1, https://doi.org/10.1007/s40891-020-0186-6.

8. W. Zou, J. Ye, Z. Han, S. K. Vanapalli, and H. Tu, "Effect of Montmorillonite Content and Sodium Chloride Solution on the Residual Swelling Pressure of an Expansive Clay," *Environment and Earth Science* 77 (2018): 677, https://doi.org/10.1007/s12665-018-7873-9.

9. M. L. Hossain, H. M. Shahin, and T. Nakai, "Enhancement of Bearing Capacity of Soft Soil Using Geosynthetics," *International Journal of GEOMATE* 17 (2019): 238–244, https://doi.org/10.21660/2019.64.67721.

10. D. J. U. Infante, G. M. A. Martinez, P. A. Arrua, and M. Eberhardt, "Shear Strength Behavior of Different Geosynthetic Reinforced Soil Structure From Direct Shear Test," *International Journal of Geosynthetics and Ground Engineering* 2 (2016): 17, https://doi.org/10.1007/s40891-016-0058-2.

11. Z. Chao, G. Fowmes, A. Mousa, et al., "A New Large-Scale Shear Apparatus for Testing Geosynthetics-Soil Interfaces Incorporating Thermal Condition," *Geotextiles and Geomembranes* 52 (2024): 999–1010, https://doi.org/10.1016/j.geotexmem.2024.06.002.

12. A. B. Cerato and A. J. Lutenegger, "Specimen Size and Scale Effects of Direct Shear Box Tests of Sands," *Geotechnical Testing Journal* 29 (2006): 507–516, https://doi.org/10.1520/GTJ100312.

13. E. M. Palmeira, "Soil–Geosynthetic Interaction: Modelling and Analysis," *Geotextiles and Geomembranes* 27 (2009): 368–390, https://doi.org/10.1016/j.geotexmem.2009.03.003.

14. G. Sukmak, P. Sukmak, S. Horpibulsuk, M. Hoy, and A. Arulrajah, "Load Bearing Capacity of Cohesive-Frictional Soils Reinforced With Full-Wraparound Geotextiles: Experimental and Numerical Investigation," *Applied Sciences* 11 (2021): 2973, https://doi.org/10.3390/app11072973.

15. P. He, L. Sun, and Z. Wang, "Direct Shear Test of Unsaturated Soil," *Earth Sciences Research Journal* 21 (2017): 183–188, https://doi.org/10.15446/esrj.v21n4.66103.

16. A. Zhussupbekov, A. Tulebekova, I. Zhumadilov, and A. Zhankina, "Tests of Soils on Triaxial Device," *Key Engineering Materials* 857 (2020): 228–233, https://doi.org/10.4028/www.scientific.net/KEM.857.228.

17. D. Kim and S. Ha, "Effects of Particle Size on the Shear Behavior of Coarse Grained Soils Reinforced With Geogrid," *Materials* 7 (2014): 963–979, https://doi.org/10.3390/ma7020963.

18. C. S. Vieira, M. L. Lopes, and L. Caldeira, "Soil-Geosynthetic Interface Shear Strength by Simple and Direct Shear Tests," in *Proceedings of the 18th International Conference on Soil Mechanics and Geotechnical Engineering* (International Society for Soil Mechanics and Geotechnical Engineering, 2013).

19. W. R. Azzam and A. Basha, "Utilization of Soil Nailing Technique to Increase Shear Strength of Cohesive Soil and Reduce Settlement," *Journal of Rock Mechanics and Geotechnical Engineering* 9 (2017): 1104–1111, https://doi.org/10.1016/j.jrmge.2017.05.009.

20. Y. Zhao, Z. Lu, J. Liu, J. Zhang, and H. Yao, "Influence of Different Infill Materials on the Performance of Geocell-Reinforced Cohesive Soil Beds," *Scientific Reports* 13 (2023): 12330, https://doi.org/10.1038/s41598-023-39580-x.

21. Z. Yang, J. Liu, R. Zhang, W. Shi, and S. Yuan, "Shear Resistance Evolution of Geogrid Reinforced Expansive Soil Under Freeze–Thaw Cycles," *Applied Sciences* 15 (2025): 5492, https://doi.org/10.3390/app15105492.

22. W. Hassan, B. Alshameri, M. N. Nawaz, and S. U. Qamar, "Experimental Study on Shear Strength Behavior and Numerical Study on Geosynthetic-Reinforced Cohesive Soil Slope," *Innovative Infrastructure Solutions* 7 (2022): 349, https://doi.org/10.1007/s41062-022-00945-2.

23. X. Chen, J. Zhang, and Z. Li, "Shear Behaviour of a Geogrid-Reinforced Coarse-Grained Soil Based on Large-Scale Triaxial Tests," *Geotextiles and Geomembranes* 42 (2014): 312–328, https://doi.org/10.1016/j.geotexmem.2014.05.004.

24. E. Botero, A. Ossa, G. Sherwell, and E. Ovando-Shelley, "Stress-Strain Behavior of a Silty Soil Reinforced With Polyethylene Terephthalate (PET)," *Geotextiles and Geomembranes* 43 (2015): 363–369, https://doi.org/10.1016/j.geotexmem.2015.04.003.

25. E. D. Evangelou, I. N. Markou, S. E. Verykaki, and K. E. Bantralexis, "Mechanical Behavior of Fiber-Reinforced Soils Under Undrained Triaxial Loading Conditions," *Geotechnics* 3 (2023): 874–893, https://doi.org/10.3390/geotechnics3030047.

26. Y. Guo, Y. Xue, Y. Zhang, et al., "Mechanical and Deformation Behavior of Silt Reinforced With Wicking Geotextile: An Experimental Study," *Construction and Building Materials* 482 (2025): 141721, https://doi.org/10.1016/j.conbuildmat.2025.141721.

27. X. Wang, Q. Hu, Y. Liu, and G. Tao, "Triaxial Test and Discrete Element Numerical Simulation of Geogrid-Reinforced Clay Soil," *Buildings* 14 (2024): 1422, https://doi.org/10.3390/buildings14051422.

28. J. Liu, J. Pan, B. Wang, C. Hu, and Q. Liu, "Study on the Shear and Deformation Characteristics of Geogrid-Reinforced Gravelly Soils Based on Large-Scale Triaxial Tests," *Frontiers in Earth Science* 12 (2024): 1–13, https://doi.org/10.3389/feart.2024.1287718.

29. N. S. Parihar, R. P. Shukla, and A. K. Gupta, "Effect of Reinforcement on Soil," *International Journal of Applied Engineering Research* 10 (2015): 4147–4151.

30. A. Soltani, A. Deng, and A. Taheri, "Swell–Compression Characteristics of a Fiber–Reinforced Expansive Soil," *Geotextiles and Geomembranes* 46 (2018): 183–189, https://doi.org/10.1016/j.geotexmem.2017.11.009.

31. Utkarsh and P. K. Jain, "Enhancing the Properties of Swelling Soils With Lime, Fly Ash, and Expanded Polystyrene: A Review," *Heliyon* 10 (2024): e32908, https://doi.org/10.1016/j.heliyon.2024.e32908.

32. S. K. Namburu, H. Venkateswarlu, and S. Kolathayar, "Experimental Evaluation of Geocoir Cell-Reinforced Sand Beds With Different Infill Materials," *International Journal of Geosynthetics and Ground Engineering* 11 (2025): 15, https://doi.org/10.1007/s40891-025-00622-1.